RUSSIAN ACADEMY OF SCIENCE

Lenin Order of Siberian Branch

G.I. BUDKER INSTITUTE OF NUCLEAR PHYSICS

I.V. Bedny, A.E. Bondar, V.V. Cherepkov,
D.A. Epifanov, M.G. Golkovsky, A.S. Kuzmin,
S.B. Oreshkin, V.E. Shebalin, B.A. Shwartz, Yu.V. Usov

STUDY OF THE RADIATION HARDNESS
OF PURE CsI SCINTILLATION CRYSTALS

Novosibirsk

2007

Study of the radiation hardness of pure CsI scintillation crystals

I.V. Bedny, A.E. Bondar, V.V. Cherepkov, D.A. Epifanov,
M.G. Golkovsky, A.S. Kuzmin, S.B. Oreshkin, V.E. Shebalin,
B.A. Shwartz, Yu.V. Usov

Institute of Nuclear Physics 630090, Novosibirsk, Russia

Abstract

This work is related to the pure CsI radiation hardness studies. Four pure CsI crystals and one counter assembled with pure CsI crystal and vacuum Hamamatsu photopentode have been studied. Both scrystalls and counter have geometric sizes of the Belle counters. Two studied samples have been irradiated with dose up to 55 krad and 3 another samples with the dose up to 13 krad. Four of studied samples is found to have high enough radiation hardness. For the dose of about 13 krad their light output decreasing is less than 15%. For one of the samples the lightoutput reduction is about 66%. Presence of such crystals requires to perform test of the radiation hardness of each crystal.

Изучение радиационной стойкости кристаллов чистого CsI

И.В. Бедный, А.Е. Бондарь, М.Г. Голковский, Д.А. Епифанов,
А.С. Кузьмин, С.Б. Орешкин, Ю.В. Усов, В.В. Черепков,
Б.А. Шварц, В.Е. Шебалин

Институт ядерной физики им. Г.И.Будкера 630090, Новосибирск, Россия

Аннотация

Данная работа посвящена изучению радиационной стойкости кристаллов чистого CsI. В рамках работы были изучены 4 кристалла и один счетчик, собранный на основе кристалла чистого CsI и вакуумного фотопентода Hamamatsu. Дозы облучения двух образцов составили 55 крад, и три образца были облучены дозой 13 крад. Для четырех образцов уменьшение световыхода при дозе облучения около 13 крад составило менее 15%, что удовлетворяет требованиям на радиационную стойкость кристаллов детектора Belle. Световыход одного из кристаллов уменьшился на 66%, что говорит о необходимости предварительной проверки радиационной стойкости кристаллов.

Содержание

1 Introduction

Experiments on B-physics and CP violation in *B*-decays have been carrying out for more than 8 years at the KEKB B-factory with the Belle detector [1]. One of the main systems of the Belle is the electromagnetic calorimeter which provides a measurement of the photon energy and angle in a wide energy range up to 9 GeV. The Belle electromagnetic calorimeter based on CsI(Tl) crystals includes barrel part and two endcaps covering the solid angle of 91% of 4π. A description of the calorimeter can be found elsewhere [1].

KEKB has the largest in the world luminosity about $1.7 \times 10^{34} cm^{-2} s^{-1}$ which can be further gained by factor more than ten according to the developed proposal of the KEKB collider upgrade [2]. High electron and positron currents ($>$10 A) assumed at the upgraded machine shall unavoidable provide an increase of the background. The main problem for the calorimeter is the pile-up noise caused by the signal and background overlapping. Especially high background is expected in the endcap calorimeter. To keep a good performance of the calorimeter and to suppress the pile-up noise, a replacement of CsI(Tl) by a scintillator with shorter decay time is required. As a solution the undoped CsI with decay time of 20 ns was chosen to be used in the endcap of the Belle electromagnetic calorimeter.

Another problem at high background conditions is a degradation of the scintillation crystals under radiation. By now the absorbed dose in endcap crystals is about 250 rad which caused about 10% of the crystal light output decrease. The expected radiation dose in the endcaps after accelerator upgrade is a factor 10-20 higher than we have at Belle now and for five years of operation it can be as much as 5 grads. A special study of the pure CsI radiation hardness is necessary to prove that these crystals are able to withstand the mentioned absorbed dose. It should be noted that the radiation hardness depends on raw material quality, technical process of crystal growing and sizes of the crystal. Some earlier studies of pure CsI radiation hardness can be found in the refs. [7, 8, 9].

This work is devoted to a study of the radiation hardness of pure CsI crystals with the sizes and shape of the Belle calorimeter counters. These

crystals were produced by the same company that had provided most of the crystals for the Belle calorimeter. The studied samples were irradiated by bremsstrahlung photons produced by the 1.5 Merv electron beam from ELVA-6 accelerator at BI NP [10]. Another feature of this work is that the absorbed radiation dose were measured with the detector based on CsI crystal, thus avoiding error-prone recalculation of this value depending on the energy deposition.

2 Crystals description

The properties of pure CsI scintillator in comparison with CsI(Tl) currently used in Belle detector are presented in the Table 1. The scintillation of pure CsI includes a fast component with the decay time of about 20 ns and maximum of emission spectrum at 300 nm, as well as a component with the decay time of about 1 μs [3], and maximum of its emission spectrum at 550 nm. The most part of pure CsI scintillation light corresponds to the fast component. Conventionally the ratio between this two components described by fast-to-total ratio (f/t). F/t is defined as the ratio of light amount collected during 100 ns from the beginning of the flash to that integrated over 1 μs. The intensity of the slow scintillation component essentially depends on the purity of the raw material and the details of growing process [4]. For studied samples f/t ratio was about 70-80%.

Таблица 1: The characteristics of CsI(Tl) and pure CsI scintillators at room temperature.

crystal	ρ, g/cm^3	X_0, cm	λ_{em}, nm	n	$N_{ph}/Merv$	τ, ns	$\frac{dN}{dT}$ at 20°C, %
CsI(Tl)	4.51	1.86	550	1.8	52000	1000	0.4
CsI	4.51	1.86	305/400	2	5000	20/1000	-1.3

As shown in the Table 1, light output of pure CsI crystal is much lower than that of CsI(Tl). Also pure CsI has more essential temperature dependence of light output at room temperature [5, 11].

Under a radiation load both light yield and transparency of the crystal can change resulting in a decrease of the counter signal as well as position nonuniformity [4]. For large CsI(Tl) crystals used in high energy physics experiments the main reason of light output degradation is the increase of the light absorption caused by the radiation [6].
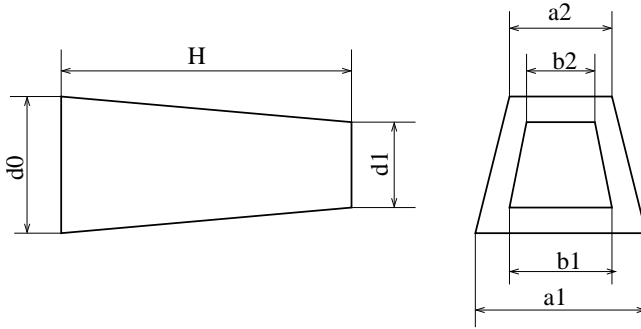
Crystal serial number	cr.1	cr.8	cr.45, 46, 122
H, mm	300	300	300
d0, mm	54	61	63
d1, mm	50	54	54
a1, mm	61	71	80
a2, mm	63	67	76
b1, mm	54	62	70
b2, mm	55	59	67

Рис. 1: CsI crystals.

The elements of the Belle calorimeter have the shape of truncated pyramid. The sizes of the samples studied in this work are shown in Fig. 1.

In this work 5 samples were studied. Four of them were pure CsI crystals while the fifth one was the assembled Belle counter prototype consisted of the pure CsI crystal connected to the vacuum photopentode. All crystals were packed in a porous teflon sheet of 100 μm and aluminized mylar layer of 50 μm. The counter layout is described in the next section. Light collection nonuniformity along crystal axis for this samples was about 10%.

Two pure CsI crystals were studied in 2004 (crystals N 1 and N 8). In 2006 new measurements were done with other two pure CsI crystals (crystals N 45 and N 122)) and one assembled counter based on pure CsI crystal (crystal N 46). All of the crystals had been produced by "Amcrys-H"ltd. corporation of "Monocrystals"scientific-technology concern (Kharkov, Ukraine).
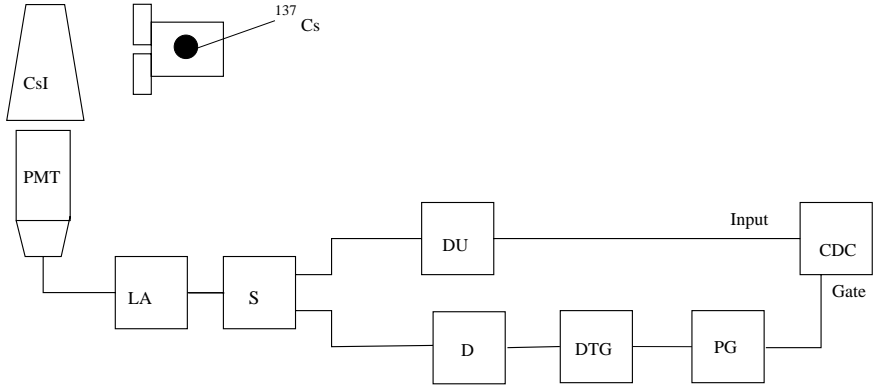
Рис. 2: The setup for light output measurements. LA – linear preamplifier, S – splitter, DU – delay unit, D – discriminator, DTG – dead time generator, PG – pulse generator.

3   Light output measurement

For light output measurements the setup presented in Fig. 2 was used. The studied crystal was irradiated by γ-quanta from a collimated ^{137}Cs radioactive source, which could move along the crystal axis. The crystal was installed on the photocathode of the photomultiplier tube (PMT) without optical contact. The signal from PMT was amplified by linear amplifier (LA) and after splitter (S) fed to the linear channel and trigger channel. The amplified signal was digitized with a charge to digital converter (CDC). In the trigger channel the discriminator, the dead time generator and the pulse generator were set. The discriminator was used to setup the threshold. Dead time generator with dead time set to 3 μs prevented the overlapping of signals. This layout had been assembled in CAMAC crate. Pulse generator provided the gate signal for CDC with changeable duration. For all crystals measurements were performed for the short component of scintillation and for total one. The gate signal duration was set to 100 ns and 1 μs for the measurement of short component and total component correspondingly.

A typical amplitude spectrum for the fast component of the signal from the PMT is shown in Fig. 3. The total energy absorption peak corresponding to 662 keV is clearly seen. The smooth substrate is caused by the Compton effect and, at lower part, by the electronics noise. In the peak region the
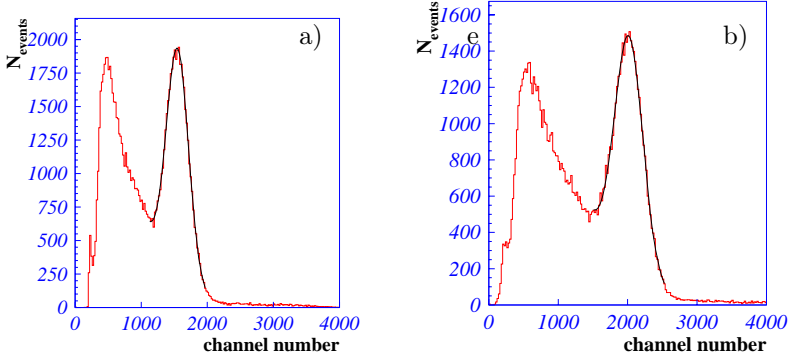
Рис. 3: The spectrum of ^{137}Cs obtained with CsI counter measuring the short component(a) and total component(b).

spectrum is approximated by the dependence:

$$f(x) = N_1 \ e^{-\frac{(A-A_0)^2}{2\sigma^2}} + N_2 \ e^{-\alpha \ A}, \qquad (3.1)$$

where the first term describes the total absorption peak while the second term approximates the substrate. The light output of the crystal is characterized by the peak position A_0. The scheme stability was monitored using the signal from a reference pure CsI crystal with the sizes of $3.5 \times 3.5 \times 3.5$ cm^3.

Moving radioactive source vertical, signal from the crystal was measured in 11 points along the crystal axis. The typical dependence of the signal from crystaln on the vertical position of the radioactive source is presented in Fig.4.
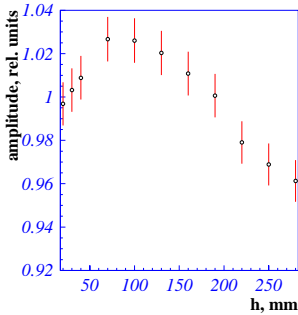

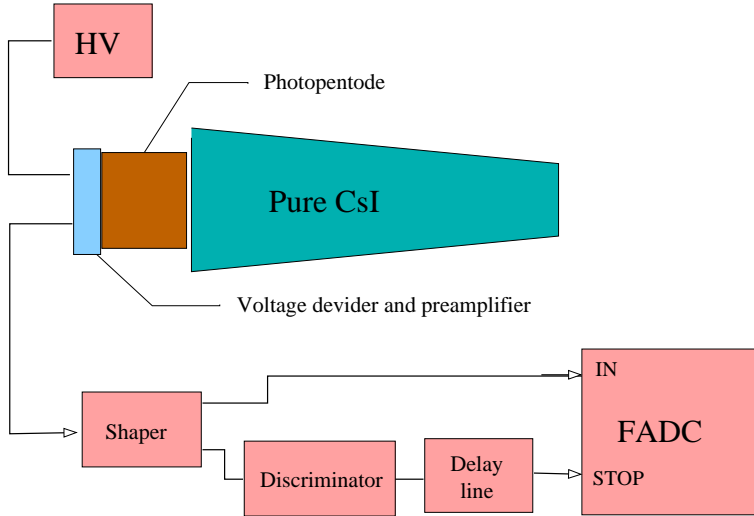Рис. 4: The light collection nonuniformity along crystal axis.

9

Рис. 5: The scheme of signals regestration from assembled counter. Signal from counter feeds to the shaper. Signal from shaper feeds to the input of flash ADC and discriminator that provide STOP signal.
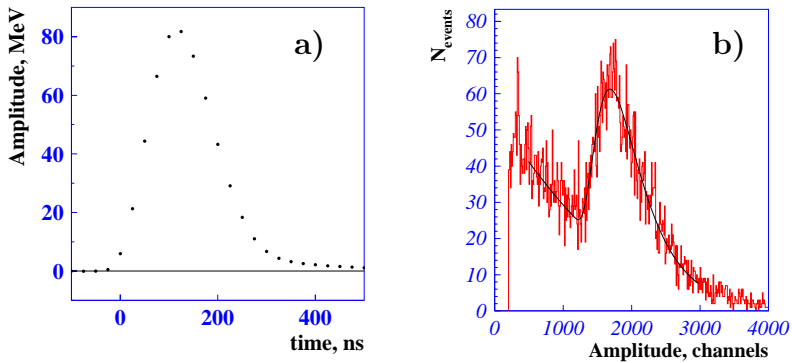

Рис. 6: The shape of the signal from counter(a) and the cosmic spectrum measured by counter(b).

The layout of the Belle scintillation counter prototype is presented in Fig. 5. To detect the light from the crystal 2"photopentode developed by Hamamatsu Photonics is used. It has been coupled with the crystal using optical grease. The signal from the photopentode comes to charge sensitive
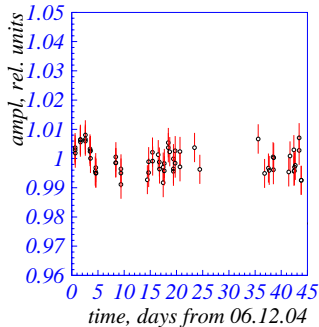
Рис. 7: The time dependencies of the reference crystal light output after temperature correction.

preamplifier of the same type as used in the present Belle counters. The output pulse from the preamplifier is applied to a shaper consisting of the differentiation stage (τ=30 ns) and two stages of the active Bessel filters of the second order [12]. The shaped signal is digitized by the flash ADC with the clock rate of 43 MHz. The digitized data are recorded to the ring buffer. The buffer readout is initiated by the trigger signal which is generated when the output pulse height exceeds the threshold which is equivalent of 4 MeV of the energy. 16 measurements around the signal maximum (Fig. 6a) are fit to the function with definite shape and two free parameters - the pulse height and the arrival time.

In order to monitor the light output of the counter the spectrum(Fig. 6b) of cosmic particles was measured. Since the counter was located horizontally, the cosmic ray muons crossing the crystal from top to bottom surfaces provide a Landau-like spectrum with the distinctive peak. The broad structure appears due to the particles crossing one of the side surfaces. Counter light output was determined by the peak position.

As it was noted above, pure CsI crystals light output depends on its temperature. Therefore the crystal temperature is measured using special sensors attached to the crystal surface and the lightoutput is corrected according to the formula (see Table 1):

$$L = L_m(1 - 0.013(t - t_0)), \tag{3.2}$$

where t – crystal temperature, t_0 – reference temperature chosen at 17°C, L_m – the measured light output. The time dependencies of the reference crystal light output without and with temperature correction are presented in Fig.7. As it is seen in the figure, accuracy of light output measuring was about 1.5%.
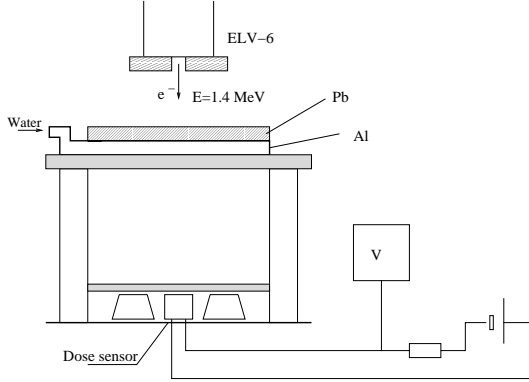
11

Рис. 8: The crystals irradiation scheme. ELV-6 provides electron beam wich produce photons in the converter (Pb). Converter is cooling by water converter. Crystals and dose sensor is located under converter. Using voltmeter V the dose sensor current is measured.

4   Crystals irradiation

The studied samples were irradiated by bremsstrahlung as shown in the Fig. 8. ELV-6 provides the electrons with the energy 1.4 MeV and beam current up to 100 mA. Bremsstrahlung γ-quanta created in the converter by the electrons, irradiate the crystals located on the horizontal surface at about 1 m distance below the converter. In order to measure dose absorbed in the crystals the dose detector [13] is placed together with the crystals. The dose rate was controlled by the beam current and accumulated dose was determined by irradiation time. The 6 mm wood plate over the crystals was used to suppress the the electrons scattered in air.

Converter is located at about 30 cm from the accelerator output. The beam diameter at the converter is about 10 cm. Due to the electron scattering in the converter material the bremsstrahlung γ-quanta beam is wide. The photon flux variation along the 30 cm crystal is not more than 10%.

The resulting photon beam has wide spectrum upto 1.4 MeV with average value around 0.6 MeV. The γ-quanta spectrum obtained by Monte-Carlo simulation using the GEANT package is presented in Fig. 9. At this energy, the average photon interaction length in CsI is about 3 cm. Since the transverse size of the crystal is about 6 cm the dose absorbed near the upper side of the crystal is a few times higher than that at the bottom one. To compensate this nonuniformity each sample was irradiated with equal doses from opposite sides.
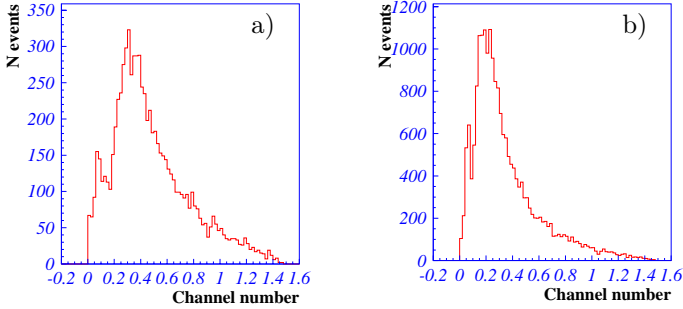
Рис. 9: The γ-quanta spectrum for lead converter case(a) and tantalum one.

For the irradiations with a dose less or about 10 krad, when the dose rate about few rad/s was sufficient (beam current <2 mA), lead converter was used. It consists of 3 mm lead plate cooled by water radiator and blown above by cooling air. In the case of doses higher than 15 krad it was necessary to increase the current up to 15 mA (dose rate of 40 rad/s) not to occupy accelerator too long. In this case the power of 20 kW is absorbed in the converter which cause melting of the lead plate. For the doses more than 15 krad so the lead converter was replaced by more refractory tantalum converter. This converter consisted of 0.5 mm of Ta, 2 mm of water and 2 mm of stainless steel. The photon spectra after converters were slightly different (Fig. 9).

5   The dose measurement

The dose (D) is an energy deposited per unit of matter mass. It depends on the γ-quanta spectrum and the material properties. In this work the dose rate was measured using the specially made sensor wich consists of a small CsI(Tl) crystal and a silicon photodiode. Thus, the dose detector is built from the same material as the studied samples (we can neglect the small ($\sim 10^{-3}$) admixture of the thallium in the detector crystal). The amount of scintillation light is proportional to the deposited energy. So, the photodetector current is proportional to the energy, deposited in the detector per time unit:

$$R = \frac{dD_{detector}}{dt} = k_{detector}I_{detector}, \qquad (5.3)$$

The $k_{detector}$ value was determined in the calibration procedure (see the

Appendix A) and it was found to be $k_{detector} = 0.119 \pm 0.010 \frac{rad \cdot s}{\mu A}$ The dose rate was determined by measurement of the $I_{detector}$.

To determine the sensor current, voltage on the resistance of R=2 kOm was measured by the voltmeter V (Fig.8). The typical time dependence of PIN-diode current during the irradiation is presented in Fig. 10(b). The gap in center of this plot corresponds to accelerator shut down for crystals rotation. The construction and calibration procedure

Рис. 10: The signal from dose sensor.

of this detector are described in Appendix A.
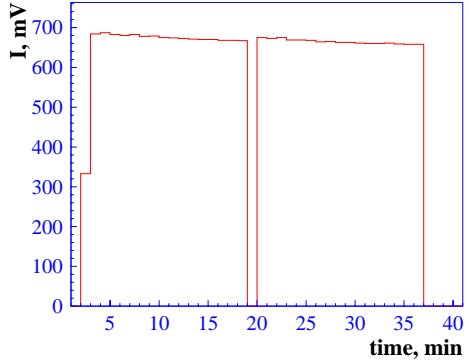
As it was noted in the previous section, the average photon interaction length in CsI is about 3 cm. Due to 6 cm thickness of the sample the absorption dose considerable changes from upper surface to the bottom one if the crystal is irradiated as show on the Fig. 8. The distribution of the dose deposition in this case obtained by the GEANT simulation is shown in Fig. 11a. To minimize the dose nonuniformity, samples were irradiated from two opposite sides. The nonuniformity in this case is presented in Fig. 11b.
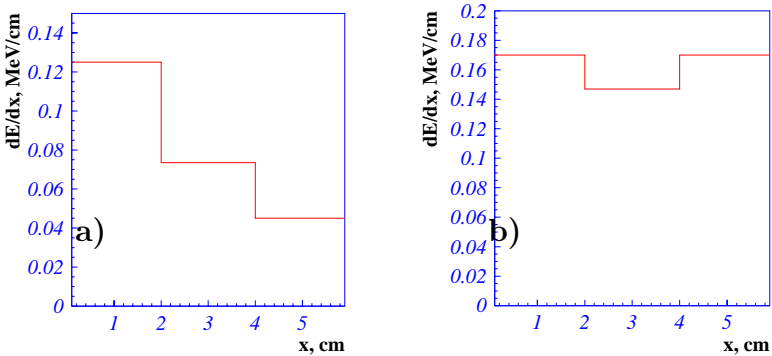

Рис. 11: The nonuniformity of the energy distribution in the crystal for irradiation from one side(a) and for irradiation from two opposite sides(b).

14

Due to the nonuniformity and different sizes of detector and samples, the average dose absorbed in the detector ($D_{detector}$) and in the sample ($D_{crystal}$) are different by the factor of k_{dose}:

$$k_{dose} = \frac{D_{measured}}{D_{crystal}}, \quad (5.4)$$

The coefficient k_{dose} was determined by the simulation. For this purpose the irradiation conditions were simulated. Two opions were considered: the lead converter (for low doses) and tantalum converter (for hugher doses). We generated initial monochromatic electrons with energy of 1.4 MeV and limulated it's interraction with converter, production of the bremsstrahlung photons. We also considered interraction of the bremsstrahlung photons with crystal samples and obtained average energy deposited in the CsI crystals per one electron interraction with a converter. k_{dose} was determined through the energy absorbed in the CsI layer of thickness $X_{detector} = 1\ cm$ and energy absorbed in the whole crystal with thickness $X_{crystal} = 6\ cm$:

$$k_{dose} = \frac{E_{detector}/X_{detector}}{E_{crystal}/X_{crystal}}, \quad (5.5)$$

The results of simulation for lead converter are $E_{detector} = 156 \pm 3 \pm 12\ keV$, $E_{crystal} = 493 \pm 10 \pm 39\ keV$. The first error is statistical and another one is systematic contributed by inconstancy of crystal thickness along crystal axis and accuracy of the setup geometry description. For the tantalum converter the corresponded energies are $E_{detector} = 143 \pm 1 \pm 10$, $E_{crystal} = 348 \pm 3 \pm 24$. Conversion coefficients are $k_{dose} = 1.89 \pm 0.13$ and $k_{dose} = 2.47 \pm 0.17$ for the lead and tantalum converters respectively. Therefore the total dose absorbed by crystal is

$$D = \int_0^T I\ dt\ k_{detector}\ k_{dose}, \quad (5.6)$$

where I - dose detector current, T - irradiation duration, k_{dose} - coefficient of recalculation of the dose absorbed in the detector to the dose absorbed in the crystal, $k_{detector}$ - the coefficient of connection between dose rate and detector current .

6   Results

Within this work two sessions of pure CsI radiation hardness studies were performed. At the first one two pure CsI crystals N1 and N8 which were irradiated five times with doses of 280, 980, 4250, 10300, 32000 rad. Parameters of irradiations are shown in Table 2. The second study was performed with two pure CsI crystals N45 and N122 and one assembled counter. In this case doses of irradiations was 890, 3200, 8500 rad, and irradiation parameters are shown in Table 3.

Таблица 2: The crystals irradiation parameters for the first study

Run number	accelerator current, μA	total dose deposited in the samples, rad	irradiation time, s	dose rate measured by the sensor, rad/s
1	200	280±30	1000	0.46 ± 0.04
2	450	980±88	2000	0.98 ± 0.08
3	800	4250±380	4200	2.0±0.2
4	1800	10340±930	5800	3.6±0.3
5	15000	32000±2900	2000	40±3

Таблица 3: The crystals irradiation parameters for the second study

Run number	accelerator current, μA	total dose deposited in the samples, rad	irradiation time, s	dose rate measured by the sensor, rad/s
1	800	890±70	1200	1.48 ± 0.12
2	800	3200±270	5000	1.56 ± 0.12
3	800	8500±820	10600	1.55±0.12

The dose was calculated according to Eq. 5.6. The crystal light output and the f/t ratio were measured before and after each irradiation. The time dependencies of the light output for all studied samples are shown in Fig. 12(a,b,c,d,e). All results are presented for the short component, for the total component all dependencies are very similar. The time of irradiation are shown by the vertical line in this figures. After each irradiation some reduction of light output is observed. Within several days light output is partially. The values of light output after recovery are plotted in dependence on the absorbed dose in the Fig. 12(f).

The studied samples light output degradation for the dose about 15 krad is shown in Table 4. Thus, four of five studied samples satisfy to the requirements on the Belle detector crystals, while one of them demonstrates
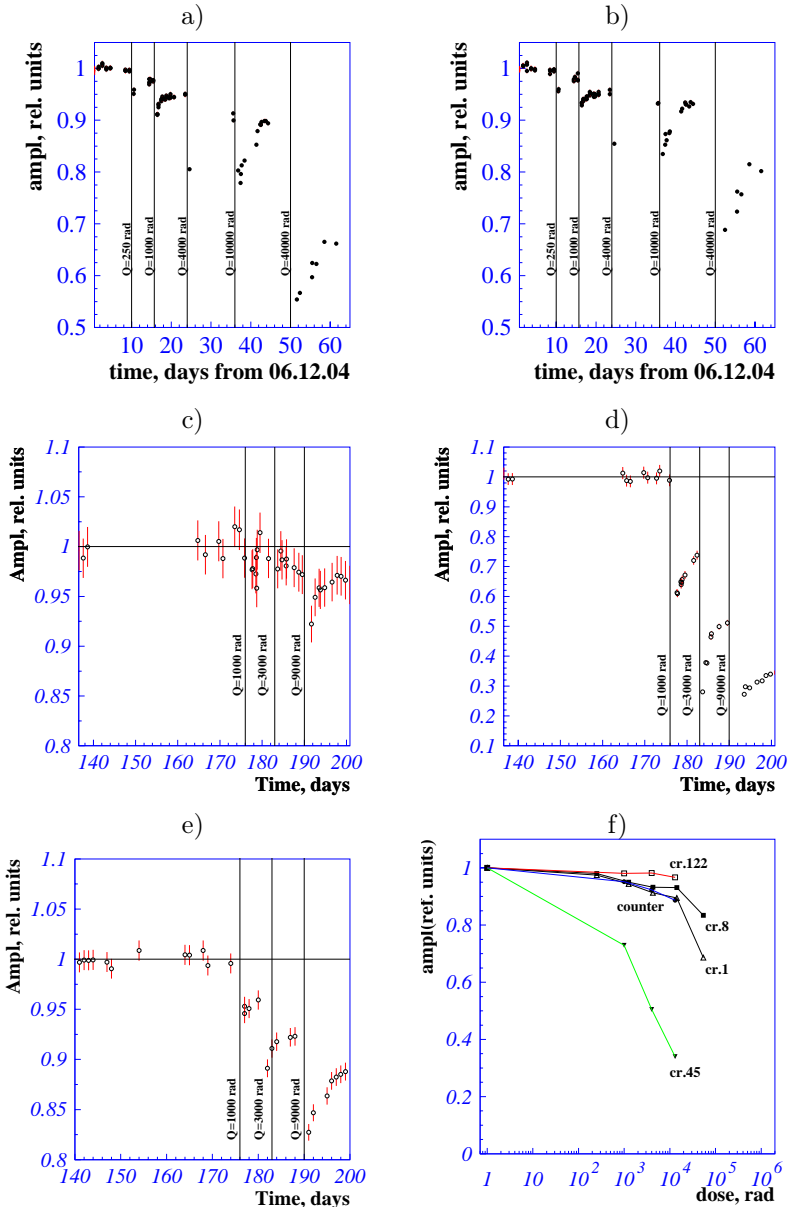
Рис. 12: The time dependencies of light output for crystal 1(a), 8(b). 122(c), 45(d) and assembled counter(e). The dependencies of crystals light output on the total irradiation dose dose(f).

17

Таблица 4: The light output decreasing for samples with absorbed radiation dose about 13 krad.

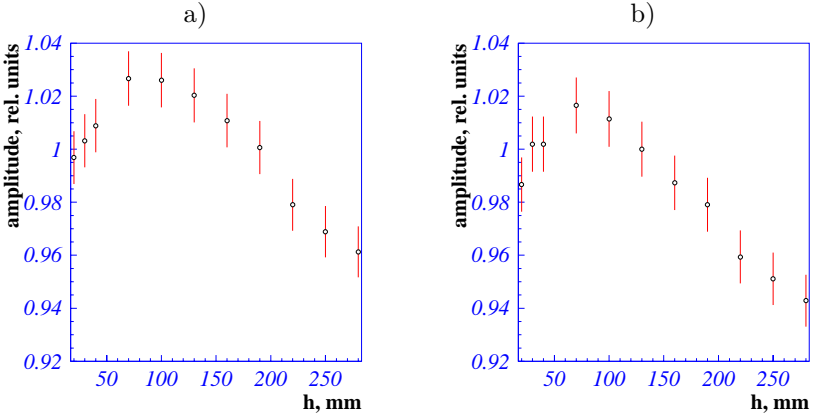| Sample	light output decreasing
1	9%
8	7%
45	66%
122	3%
counter	11%

Рис. 13: The light collection nonuniformity along crystal axis before(a) and after(b) irradiations.

the poor radiation hardness. It means that each crystal should be checked for the radiation hardness before counter assembling.

No changes of fast to total ratio within experimental accuracy of 3% was observed.

The light collection nonuniformity along the crystal axis was also measured. For this purpose collimator was moved along crystal axis and light output was measured in 11 points. The obtained results are shown in Fig. 13. The light collection nonuniformity coefficient is determined as:

$$G = \frac{L_{max} - L_{min}}{\bar{L}}, \qquad (6.7)$$

where L_{min} and L_{max} – minimum and maximum values of the light output,

18

$\bar{L}$ – the average light output along the crystal axis. The nonuniformity of all crystals was less than 10%. The total nonuniformity changes was less than 3% that is within the experimental error.

7 Conclusion

This work was related to the pure CsI radiation hardness studies. Four pure CsI crystals and one counter assembled with pure CsI crystal and vacuum Hamamatsu photopentode were studied. Both scrystalls and counter had geometric sizes of the Belle counters. Two studied samples were irradiated with dose up to 55 krad and 3 another samples with the dose up to 13 krad. Four of studied samples were found to have high enough radiation hardness. For the dose of about 13 krad their light output decreasing was less than 15%. For one of the samples the lightoutput reduction was about 66%. Presence of such crystals pointed to test the radiation hardness of each crystal.

A Dose detector calibration

Construction of the dose detector is shown in Fig. 14. This detector consists of CsI(Tl) crystal of sizes of $1 \times 2 \times 2$ cm^3 coupled with optical contact with semi-conductor photodiode S2744-08. One more photodiode was placed behind of the first photodiode without light connection with the crystal. During irradiation the part of the energy is absorbed in the PIN-diode
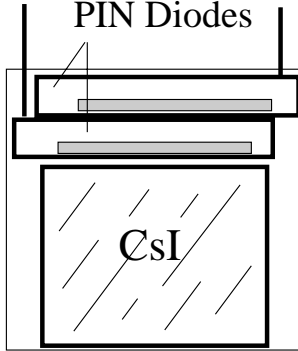

Рис. 14: The dose detector based on the CsI(Tl) crystal and two PIN-diodes.

volume resulting in increase of the dark current. The second photodiode allows to take into account this effect. During irradiation the currents of both photodiodes were recorded and difference was considered as the signal current. The addition photodiode current was about 2% of the photodiode mounted on the crystal.

The dose rate Q absorbed in the detector is proportional to the detector current, and can be described through average energy deposition $\bar{E}$, frequency ν of the signals from detector, and crystal mass M:

$$Q = k_{detector} I_{detector} = \frac{\bar{E}\nu}{M}, \tag{A.8}$$

the coefficient $k_{detector}$ is the calibration coefficient should be determined for calibration.

The ^{60}Co source was used to calibrate the detector. Measuring the spectrum(15a) from ^{60}Co radioactive source the average energy deposition in the crystal was determined. Average energy was determined by spectrum(15c) after noise spectrum(15b) subtraction. Then using measured
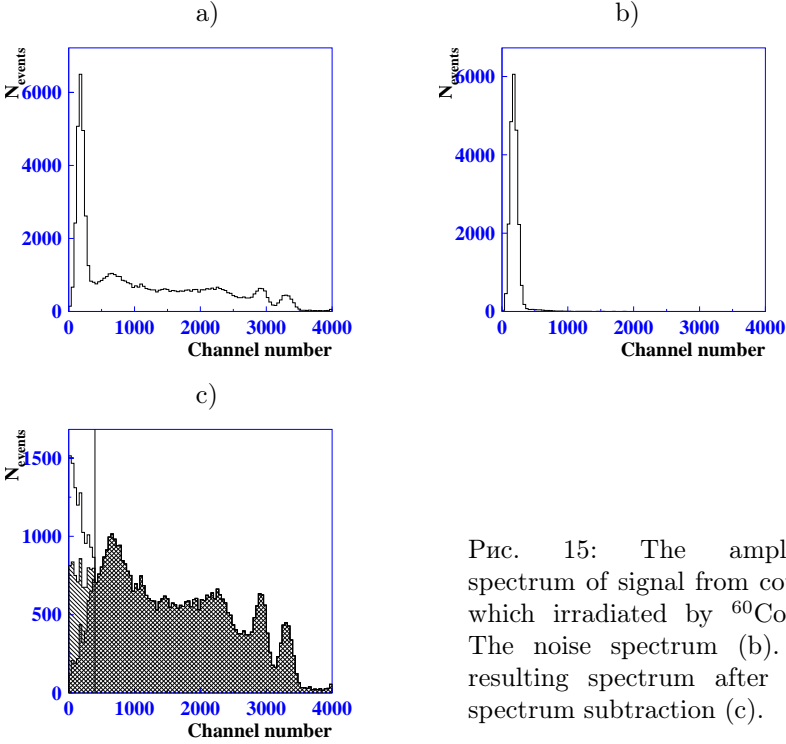
a) b)

c)

Рис. 15: The amplitude spectrum of signal from counter which irradiated by ^{60}Co (a). The noise spectrum (b). The resulting spectrum after noise spectrum subtraction (c).

values of signals frequency, and detector current, and known crystal mass the $k_{detector}$ was determined:

$$k_{detector} = \frac{\bar{E}\nu}{I\,M} = 0.119 \pm 0.010 \frac{rad/s}{\mu A}. \tag{A.9}$$

The main contribution to the accuracy is the error of the ν calculating and average energy absorption determining(7%). In general the $\bar{E}$ measuring precision is determined by error of subtracting noise spectrum from total one. Resulting spectrum was obtained as:

$$N_i = N_{0\,i} - N_{noise\,i} \frac{T_{signal}}{T_{noise}}, \tag{A.10}$$

where N_i – the number of the detector responses in i-th ADC channel, T_{signal} – the duration of signal spectrum measuring, and T_{noise} – duration of noise

21

spectrum measuring. The error of $\frac{T_{signal}}{T_{noise}}$ was 4%, and it's contribution to the calibration coefficient error was 1.6%. The error due to the spectrum reconstruction is 1.3% (Fig. 15(c)). Resulting estimation of the dose detector calibration error is 8.3%.

For the same accelerator parameters the new and old detectors data were in agreement within error of about 10% which is in consistent with beam reproducibility of ELV.

Список литературы

[1] A.Abashian *et al.*, The Belle detector., Nucl. Inst. &Meth., A479, 117 (2002).

[2] Letter of Intent for KEK Super B Factory. KEK Report 2004.

[3] Schotanus P. *et al.*, Scintillation characteristics of pure and Tl-doped CsI crystals, IEEE Trans. Nucl. Sci., 1990, NS-37, N2, p.177-182.

[4] Globus M.E., Grinyov B.V., Inorganic scintillators (in Russian), Akta, Kharkov, 2000.

[5] Bedny I. *et al.*, Csi Test Beam study, to be published.

[6] Beylin D. M., *et al.*, Study of the CsI(Tl) radiation hardness (in Russian), Novosibirsk, 2003.

Beylin D. M., *et al.*, Study of the radiation hardness of CsI(Tl) scintillation crystals., Nucl. Inst. &Meth., A541, 501-515 (2005).

[7] Skwarnicki T. *et al.*, Readout techniques and radiation damge of undoped cesium iodide, IEEE Trans. Nucl. Sci., 1990, NS-37, N2, p492-499.

[8] Woody C.L. *et al.*, Radiation damage in undoped CsI and CsI(Tl), IEEE Trans. Nucl. Sci., 1992, Vol.39, N4, p.524-531.

[9] Shiran N.V. *et al.* Radiation damage and afterglow of fast CsI-type scintillators, Nucl. Trans. Radiat. Meas., 1993, Vol.21, N1, p.107-108.

[10] Golubenko Yu.I. *et al.*, BINP preprint 97-7, Novosibirsk, 1997.

[11] Amsler C. *et al.*, Temperature dependence of pure CsI: scintillation light yield and decay time, Nucl. Instr. and Meth. in Phys. Res., A 480 (2002) 494-500.

[12] A. N. Vinokurova, Bachelor tethesis, BINP, Novosibirsk 2004.

[13] V. E. Shebalin, Bachelor tethesis, BINP, Novosibirsk 2005.

I.V. Bedny, A.E. Bondar, V.V. Cherepkov, D.A. Epifanov,
M.G. Golkovsky, A.S. Kuzmin, S.B. Oreshkin, V.E. Shebalin,
B.A. Shwartz, Yu.V. Usov

Study of the radiation hardness
of pure CsI scintillation crystals

И.В. Бедный, А.Е. Бондарь, М.Г. Голковский, Д.А. Епифанов,
А.С. Кузьмин, С.Б. Орешкин, Ю.В. Усов, В.В. Черепков,
Б.А. Шварц, В.Е. Шебалин

Изучение радиационной стойкости кристаллов
чистого CsI

Budker INP 2007-27